Proposed Biomedical Applications of Zirconium-Based Metal-Organic Frameworks as Drug Delivery Systems

2019

Ariel Margaret Perry-Mills
University of Central Florida

PROPOSED BIOMEDICAL APPLICATIONS OF ZIRCONIUM-BASED METAL-ORGANIC FRAMEWORKS AS DRUG DELIVERY SYSTEMS

by

ARIEL MARGARET PERRY-MILLS

A thesis submitted in fulfillment of the requirements
for the Honors in the Major Program in Biomedical Sciences
in the Burnett School of Biomedical Sciences
and in the Burnett Honors College
at the University of Central Florida
Orlando, Florida

Spring Term 2019

Major Professors: Fernando Uribe-Romo and Robert Borgon

ABSTRACT

Metal-organic frameworks (MOFs) are a class of highly crystalline nanoporous materials that self-assemble from inorganic metal oxide clusters and multitopic organic linkers. MOFs can be altered in terms of the types of metals and structures of organic linkers used, allowing for a high degree of customization and manipulation of the synergistic chemical or physical properties that arise from the precise coordination of their molecular components, including exceptionally large surface area and pore size. Zirconium-based MOFs, called UiOs in honor of their conception at the University of Oslo, also show remarkable chemical stability in both acidic and basic environments, making them excellent candidates for biomedical applications as drug delivery systems, where they can either function as molecular cargo ships, with drugs packed into their pores, or as controlled release systems, in which drug molecules are directly attached to their ligands for precise delivery. The objective of this work is to prepare water-stable MOFs whose linkers are decorated with functional groups that have potential compatibility in drug delivery systems and to explore the efficacy of certain synthesis conditions in terms of the crystallinity of the MOF product. Thus, we hope to establish a basis for the ligation of anticancer drugs and fluorescent tags to MOFs for their controlled release at a specified location within the body. These targeted release mechanisms represent new therapeutic possibilities in terms of cancer treatment as their specificity would mitigate damage to healthy tissues, thereby addressing one of the greatest weakness of present treatment options.

TABLE OF CONTENTS

CHAPTER ONE: INTRODUCTION

Cancer

Cancer is a general term that describes a disease process by which healthy cells abnormally develop into tumor cells that display disrupted cellular function, abnormal cell division and growth, and the ability to metastasize to other tissues. Affected cells then interfere with the metabolic function of the organ systems of which they are a part, resulting in a wide variety of disease states that differ depending on the areas being affected and the extent of tumor growth. Cancer arises due to interactions between individual genetic factors and external carcinogens, which can be physical (radiation), chemical (toxins or contaminants), or biological (infection from certain pathogens) in nature. Cancer is the second leading cause of global mortality, causing approximately 16% of all deaths, and one of the leading causes of morbidity.[1] Furthermore, diagnoses are expected to increase globally by 70% over the next two decades.[1]

Current Clinical Treatments for Cancer

Current clinical treatments for cancer take many forms and often involve a multidimensional approach that incorporates two or more techniques in an effort to cure their unique cancer and temper both the symptoms associated with the disease itself and the symptoms associated with the treatments, which, due to their aggressive nature, often carry adverse side effects. Treatments are chosen based on each individual case and can take the form of surgery, radiation therapy, chemotherapy, immunotherapy, targeted therapy, hormone therapy, stem cell transplants, and precision medicine.[2] Aspects of cancer such as tumor cell heterogeneity, which describes diversity of cancer cells due to heterogeneous protein function within a given tumor, pose threats to the success of targeted cancer treatments. A given drug may destroy only the cells

identified in a primary biopsy, allowing histologically different, unnoticed cells to flourish in a form of tumor adaptation and reemergence.[3] Challenges to treatment primarily arise from the unique nature of each cancer case. Strategies such as targeting actionable alterations in oncogenetic cancers and immunobiological treatments are showing promise, although they are limited by heterogeneity and acquired resistance to treatment. Based on these factors, it is thought that a multifaceted approach comprised of various forms of precision medicine will prove to be most effective in cancer treatment.[4] At present, chemotherapy, radiation therapy, and surgery remain the most common forms of cancer treatment.

Nanomedicine

Nanomedicine, which encompasses a wide range of specific drug-delivery systems, is emerging as a promising targeted cancer treatment option as it is capable of both improving the efficacy of the delivered anticancer drugs and reducing detrimental side effects of the drugs on normal, healthy tissues. Nanomedical drug delivery systems can take the form of passive drug delivery, which relies on the buildup of a given anticancer drug in a specific area, or active drug delivery, in which the drug release is mediated by molecular recognition[5]. Metal-organic frameworks represent a new realm of possibility for nanomedicine due to their extreme customizability, which could include cancer treatments requiring specialized drug delivery vessels[6].

Metal-Organic Frameworks

Metal-organic frameworks (MOFs) are a class of crystalline nanoporous materials that are self-assembling structures consisting of inorganic metal clusters and highly customizable organic ligands that serve as linkers between the inorganic clusters in the structure.[6] MOFs can be altered via the identity, geometry, functionality, and size of their components, making them highly

customizable, with more than 20,000 unique MOFs having been reported and studied between 2003 and 2013.[7] According to Roswell and Yaghi, for a compound to be classified as a MOF, the compound must have strong bonding that provides robustness and stability, linkers that are available for modification via organic synthesis, and a geometrically well-defined structure, implying high crystallinity. These characteristics are essential to fulfill the purpose of a MOF: the exhibition of a desired synergistic chemical or physical properties arising from the precise coordination of its molecular components.[8] MOFs have extremely high surface areas, ranging from 1,000 to 10,000 m^2/g depending on their chemical composition. This is directly linked to their exceptionally large pore sizes of up to 2 nm, making them excellent molecular carriers and transporters. Composed entirely of strong bonds via reticular synthesis, MOFs exhibit extreme thermal and chemical stability, remaining stable at temperatures ranging from 250˚C to 500˚C. Research into metal-organic frameworks (MOFs) has begun to explore the possibilities of using MOFs as anticancer drug delivery materials due to the tunability of their pore size and the possibility for almost limitless customization of linker functional groups.[6,7,9]

UiO MOFs

The Zr(IV)-based UiO series of MOFs, which show stability in highly acid (pH 1) environments as well as highly basic environments (pH 14), have been shown to be biomedically compatible, exhibiting low toxicity and being readily taken up by somatic cells.[7,9] As a result of their stability, low toxicity, high surface area, large pore size, and extreme customizability, UiO MOFs are prime candidates for medical applications as drug-delivery systems, either as molecular cargo ships with drugs packed directly into their pores or as controlled release systems in which drug molecules are directly attached to their ligands for precise, directed release.[6,10] The objective of this work is to synthesize water-stable UiO MOFs whose functional groups show promise as

potential components of future drug delivery systems and to determine the synthesis conditions that most favor their successful crystallization, specifically the crystallization of MOFs containing the linkers shown in Figure 2.

CHAPTER TWO: METHODS

MOF Crystallization

The standard synthesis of metal-organic frameworks is a solvothermal crystallization reaction requiring a metal source, an acid, elevated temperatures, and sufficient time for the reaction to take place, as shown in Figure 1. The result is the formation of the crystalline matrix of the UiO-66 MOF. Figure 1 shows one unit cell of which there are many continuously repeating within any given MOF particle, forming a continuous network of space-filled cells.

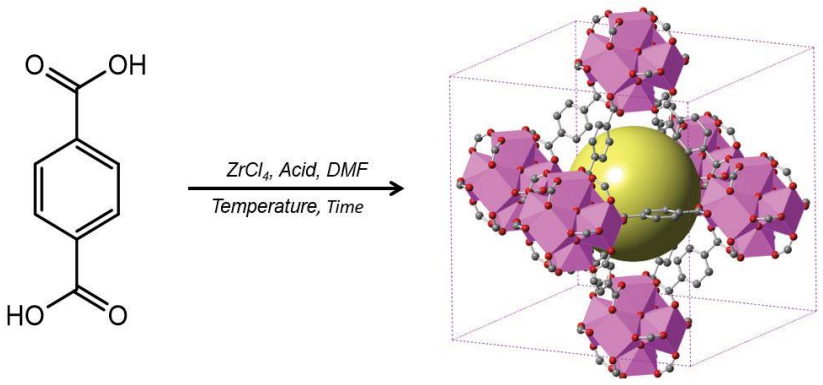

Figure 1: Standard UiO-66 MOF crystallization indicating the general materials and conditions required for such a reaction to be carried out. The yellow sphere illustrates the open space present within the center pore of the compound.

Linkers

The linkers selected, shown in Figure 2, are of varying stability and reactivity, and provide the possibility of pre- or post-synthetic substitution or modification with the exception of linker (a) which forms the unadorned UiO-66, the most fundamental UiO-MOF, illustrated in Figure 1. The linkers containing a single central phenyl ring result in the formation of UiO-66-type compounds, while the terphenyl linkers result in the formation of UiO-68-type compounds according to the standard naming conventions of UiO-MOFs.[7]

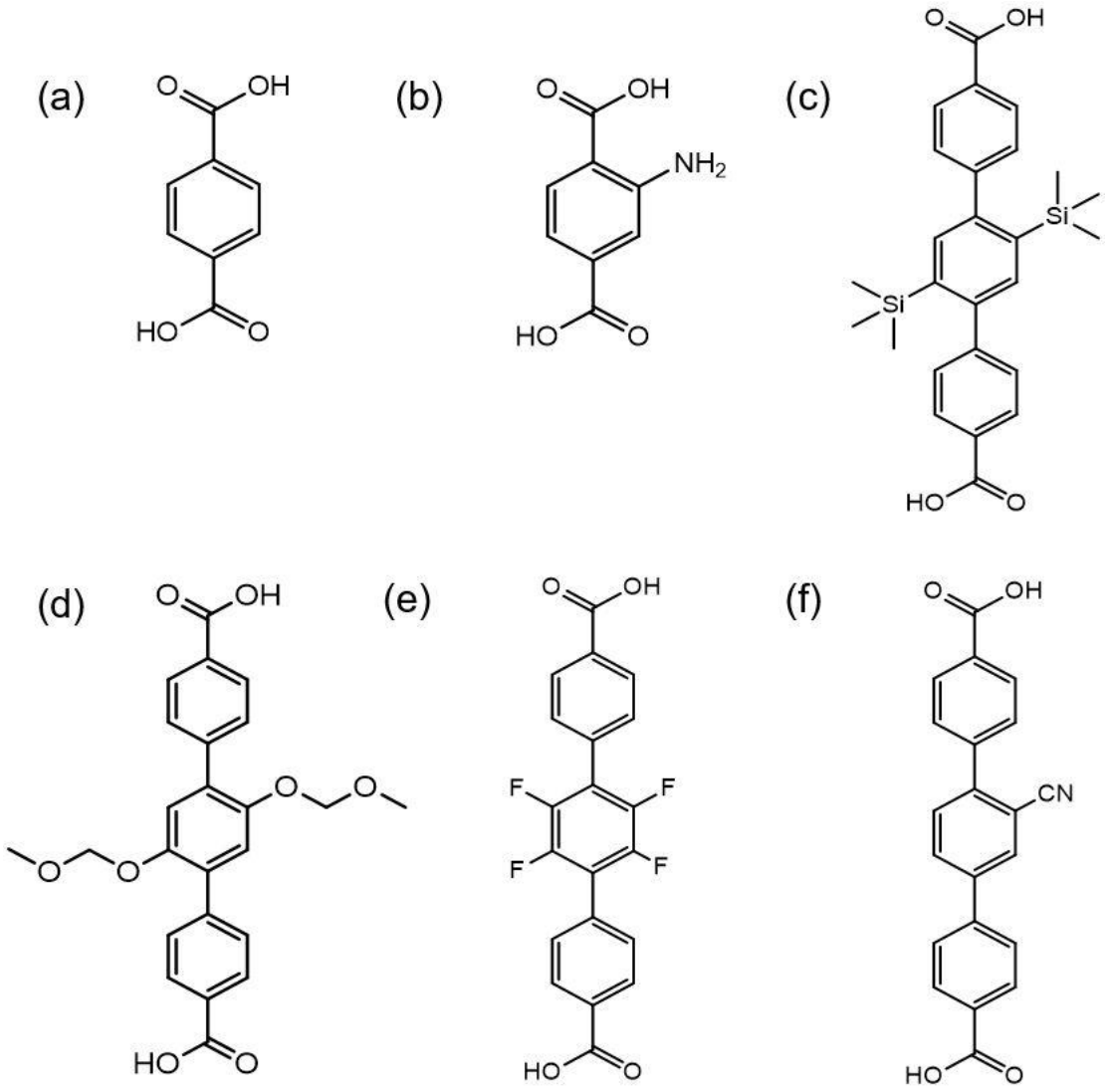

Figure 2: Organic linkers used: (a) *p*-carboxybenzoic acid linker, crystallizes to UiO-66; (b) amino linker, crystallizes to UiO-66-NH_2; (c) di-trimethylsilyl linker, crystallizes to UiO-68-TMS_2; (d) di-OMOM linker, crystallizes to UiO-68-$OMOM_2$; (e) tetra-fluoro linker, crystallizes to UiO-68-F_4; (f) cyano linker, crystallizes into UiO-68-CN.

Reaction Conditions

The reaction conditions, as defined in Table 1, were selected based upon previous experiments conducted within the laboratory in which this work was completed as being those that would be most likely to include an optimal set of conditions for each MOF being synthesized. This is necessary given that the presence of pre-synthetic functional groups is known to affect the

success of synthesis, and that by using a variety of synthetic methods, one is more likely to derive success from at least one set of conditions.

Acid	Equivalents (EQ)	Temperature	Time	Linker to Metal Cation Ratio	Metal Source
BzOH	15	120 ˚C	4 days	1:1	$ZrCl_4$, DMF
	25				
AcOH	120				
	200				
L-Proline	2.5				
	5				
TFA	15				
	25				

Table 1: Reaction conditions for crystallization.

All reactions were carried out over the course of the 4 days in flame-sealed, air-free seal tubes. Following removal from the oven, the tubes were allowed to cool to room temperature before being cut open and filtering the product over nylon.

Analysis

The compounds were analyzed for crystallinity via a powder X-ray diffraction (PXRD) and for structural integrity via Fourier-transform infrared spectroscopy (FTIR).[11,12]

CHAPTER THREE: RESULTS

PXRD Data

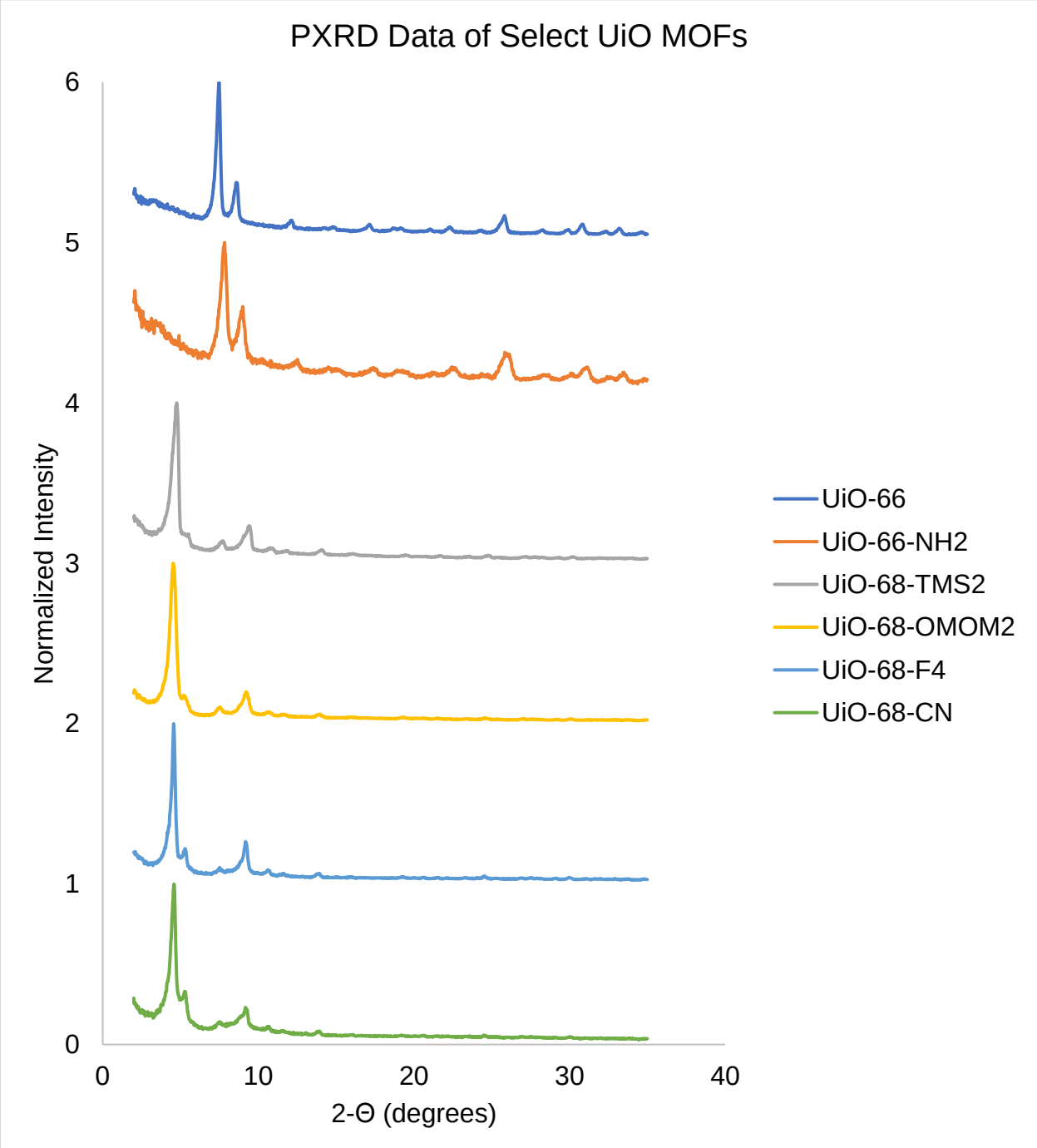

Figure 3: PXRD data from successful syntheses of select UiO MOFs under optimal reaction conditions demonstrating clear crystallinity.

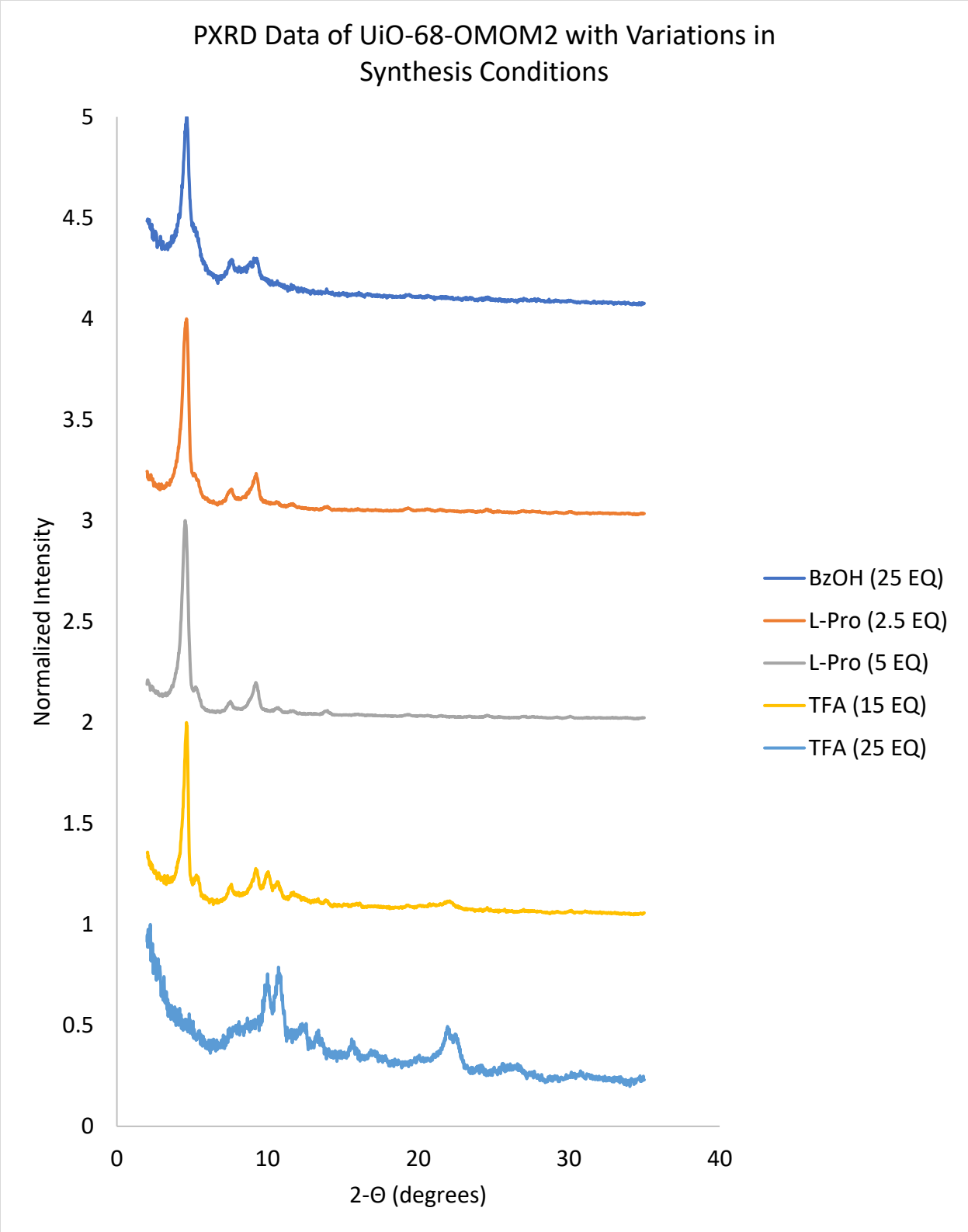

Figure 4: PXRD data from UiO-68-OMOM$_2$ products resulting from varying synthesis conditions as specified.

Physical Appearance

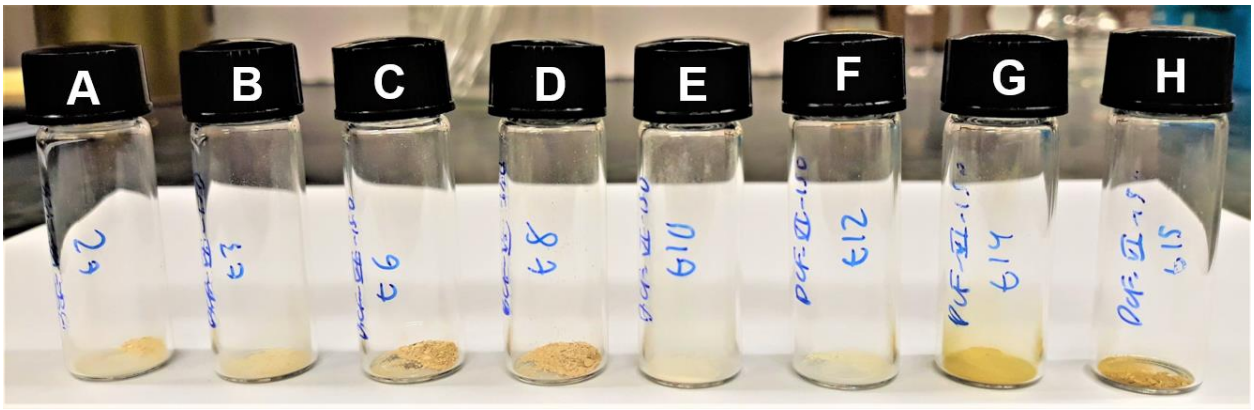

Figure 5: Powdered UiO-68-$OMOM_2$ products resulting from synthesis conditions as defined in Table 2.

Label	Acid	EQ
A	BzOH	15
B	BzOH	25
C	AcOH	120
D	AcOH	200
E	L-Proline	2.5
F	L-Proline	5
G	TFA	15
H	TFA	25

Table 2: Key to Figure 5, indicating the acid used during synthesis and its concentration.

FTIR Data

(a)

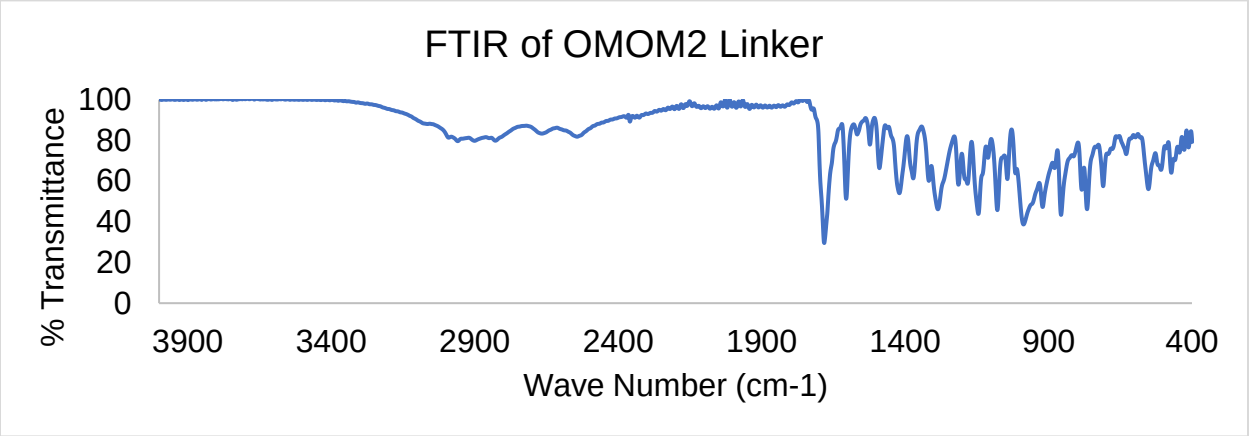

(b)

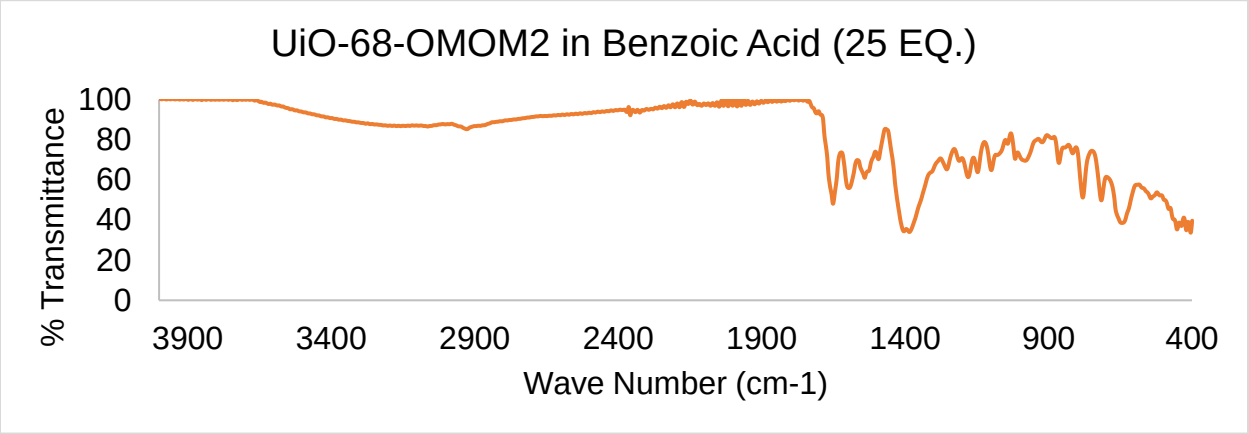

(c)

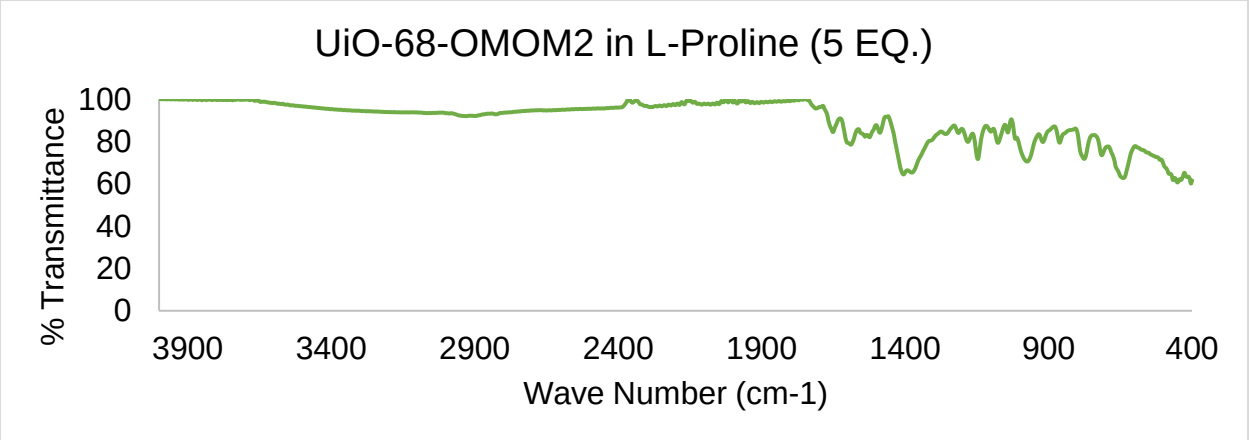

Figure 6: FTIR data from (a) $OMOM_2$ linker, (b) UiO-68-$OMOM_2$ in BzOH (25 EQ), and (c) UiO-68-$OMOM_2$ in L-Proline (5 EQ).

CHAPTER FOUR: DISCUSSION

The purpose of the work was to determine whether or not the variety of functional groups shown in Figure 2 could be successfully incorporated into MOFs, thereby laying a foundation for the additional attachment of drug groups for release within the body upon specific stimulation.

UiO-66 and UiO-66-NH_2 were synthesized according to standard protocols as defined in the literature and here serve as examples of the desired PXRD readings of UiO-66-type compounds.[13] The peaks shown in the PXRD data in Figure 3 are consistent between the two compounds, indicating the formation of identical unit cells within both compounds. Therefore, the incorporation of the amino group did not disrupt formation of the MOF and was successfully incorporated.

The UiO-68-TMS_2 whose data is shown in Figure 3 was synthesized via a solvothermal reaction under the conditions defined in Table 1 in which the acid used was L-proline at a concentration of 2.5 EQ. The product consisted of white crystals with a dull sheen, and the yield was 68.9%. The PXRD data in Figure 3 shows an initial peak at an angle that is lower than that of the initial peaks of the UiO-66-type MOFs. This difference arises as a result of the increased length of the terphenyl linkers in the UiO-68-type MOFs as compared to the shorter single-ring linkers in the UiO-66-type MOFs, and is reflected across all of the UiO-68-type MOFs shown.

The UiO-68-F_4 and UiO-68-CN whose data are shown in Figure 3 were both synthesized via a solvothermal reaction under the conditions defined in Table 1 in which the acid used was TFA at a concentration of 25 EQ. The products consisted of white powders in both cases, and the yields were 60.2% and 54.5% respectively. The PXRD data reflects a unit cell structure identical to that of the other UiO-68-type MOFs shown, indicating good crystallinity and confirming the

lack of disruption to the structure despite the incorporation of the different functional groups.

The UiO-68-$OMOM_2$ whose data is shown in Figure 3 was synthesized via a solvothermal reaction under the conditions defined in Table 1 in which the acid used was L-proline at a concentration of 5 EQ. The product was a white powder that can be seen in Figure 5F, and the yield was 66.0%. The PXRD data reflects a unit cell structure identical to that of the other UiO-68-type MOFs shown, indicating good crystallinity and confirming the lack of disruption to the structure despite the incorporation of the OMOM functional group. The FTIR data from this compound is shown in Figure 6c, which shows a distinctly different FTIR pattern from that of Figure 6a which is the reading from the $OMOM_2$ linker alone, shown in Figure 2d. The comparative intensity of the carbonyl peak at 1700 cm^{-1} to the broad peak that extends throughout the 3400 cm^{-1} to 2400 cm^{-1} region between the two FTIR images will indicate the proportion of OMOM groups that were retained throughout the synthesis, although the visible differences do indicate that the compounds are distinct from one another and there does appear to be a distinct loss of the peak intensity at 1700 cm^{-1} which could indicate that there is not free linker in the product and that the linker is well incorporated into the product.

All of the UiO-68-$OMOM_2$ products whose data is shown in Figure 4 were synthesized via a solvothermal reaction under the conditions defined in Table 1 and the acids and concentrations used are there defined within the legend of Figure 4. All reactions resulted in a 66.0% yield. The 5 EQ L-proline product showed the best crystallinity as there is minimal noise across the entirety of the reading and the peaks are clearly defined, hence it being included in Figure 3 as the ideal UiO-68-$OMOM_2$ product for comparison against the other MOFs synthesized. The 2.5 EQ L-proline product is decent, although not quite as clean as that of the 5 EQ L-proline product. The color of both products is effectively the same. The 15 EQ TFA product shows a strong initial peak,

but appears to develop patterns seen in the 25 EQ TFA product, which was not a success as it shows no initial peak and shows overall disorganization and lack of crystalline structure. Therefore, the 15 EQ TFA product may represent an incomplete synthesis with some starting materials present or a product that represents a reaction past the desired end-product, as seen in the completely degraded 25 EQ TFA product. Both TFA products show a strong yellow tone, which may be the color of the undesired product present (Figure 5G-H). Similarly, the 25 EQ benzoic acid product shows a somewhat less pronounced initial peak and the beginnings of the patterns seen in the 25 EQ TFA product, possibly indicating the same issues seen in the 15 EQ TFA product but with less MOF produced overall, resulting in the decrease of that initial peak's intensity. This is reflected in the FTIR data in Figure 6b, which illustrates an intermediate reading between that of the linker (Figure 6a) and the ideal synthesis product (Figure 6c). Therefore, it is likely that the reaction did not proceed to completion, which could explain the creamy yellow color of the product as seen in Figure 5B.

The PXRD data, FTIR data, and the physical differences in appearance between the UiO-68-$OMOM_2$ products indicate the degree of success of the various synthesis conditions in successfully incorporating the linker into a functional, crystalline MOF. It is apparent that the different acids and concentrations used do have an immediate impact upon the success of the synthesis, and that ideal conditions for different types of functional groups are different, as the differences in synthesis conditions for the MOFs whose data are displayed in Figure 3 indicate. The regularity of that data does indicate successful incorporation of all of the functional groups shown in Figure 2 into MOFs, and serves to reaffirm the importance of defining synthesis conditions for each type of functional group incorporated as there are differences amongst conditions used, as was illustrated in the differences between UiO-68-$OMOM_2$ products. This data

affirms the need for determination of ideal synthetic conditions if MOF synthesis as one of the earliest steps in the complete creation of covalent MOF drug delivery systems such that developed synthesis protocols are efficient and result in the creation of the purest and most functional product possible. In terms of the covalent attachment of the drugs themselves, the variety of functional groups used represent many possibilities for pre- and post-synthetic covalent drug attachment.

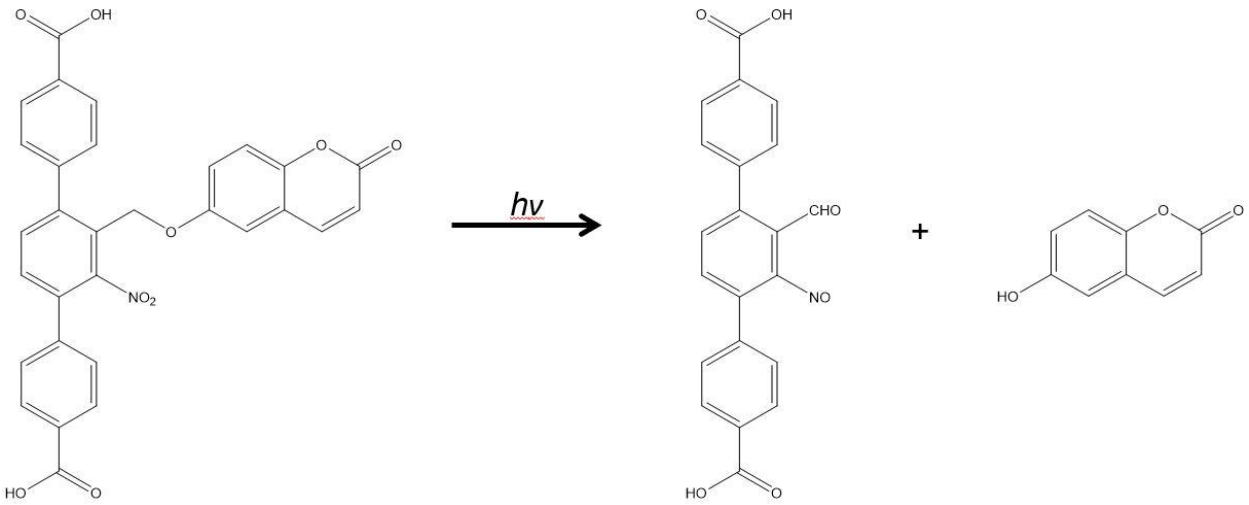

Figure 7: Proposed *ortho*-nitrobenzyl caging reaction involving the release of 7-hydroxycoumarin from a terphenyl linker that would be incorporated into a UiO-68-type MOF.

One such proposed mechanism involving pre-synthetic attachment is the light-triggered *ortho*-nitrobenzyl (oNB) caging reaction, a photocatalytic process driven by exposure to UV light. The UV light catalyzes the reaction such that the oNB group undergoes excited-state intramolecular hydrogen transfer (ESIHT) with a hydrogen on the α-carbon on the adjacent "corner" of the benzene ring, resulting in electron redistribution in which a "cage" forms between the α-carbon and nitrogen and the effector group adjacent to the α-carbon is released (uncaged), as shown in Figure 7.[14,15] Such a method would allow a given drug group to be released upon specific stimulation by UV light, allowing for selective targeting of the area of the body in which the drug would be released as determined by the area of light exposure. This method of release is made all

the more feasible by the body's ability to interact with UiO MOFs without risk of toxicity and by the MOFs ability to be introduced into the body system as either a nanoparticulate liquid suspension or in a powdered form as is typically seen immediately following synthesis.[9]

A proposed synthesis of this compound was devised as depicted in Figure 8, and work was begun on the reaction 1.1 within the synthesis in which a formylation reaction results in the attachment of an aldehyde functional group to the dibromobenzene ring. The reaction itself proved to be difficult to successfully perform and consistently produced yields below 20%. Due to time constraints for the completion of this research project, the results of this work will not be discussed here, but instead are being pursued by organic synthesis collaborators and will be reported in future publications. Nonetheless, a drug delivery mechanism capable of drug release upon UV light exposure would only release the drug upon UV light stimulation and would not result in the sort of disparate dispersal throughout the tissues seen in current chemotherapeutic treatments, thereby avoiding collateral damage of healthy tissues as non-activated MOF particles would simply pass through the body intact.

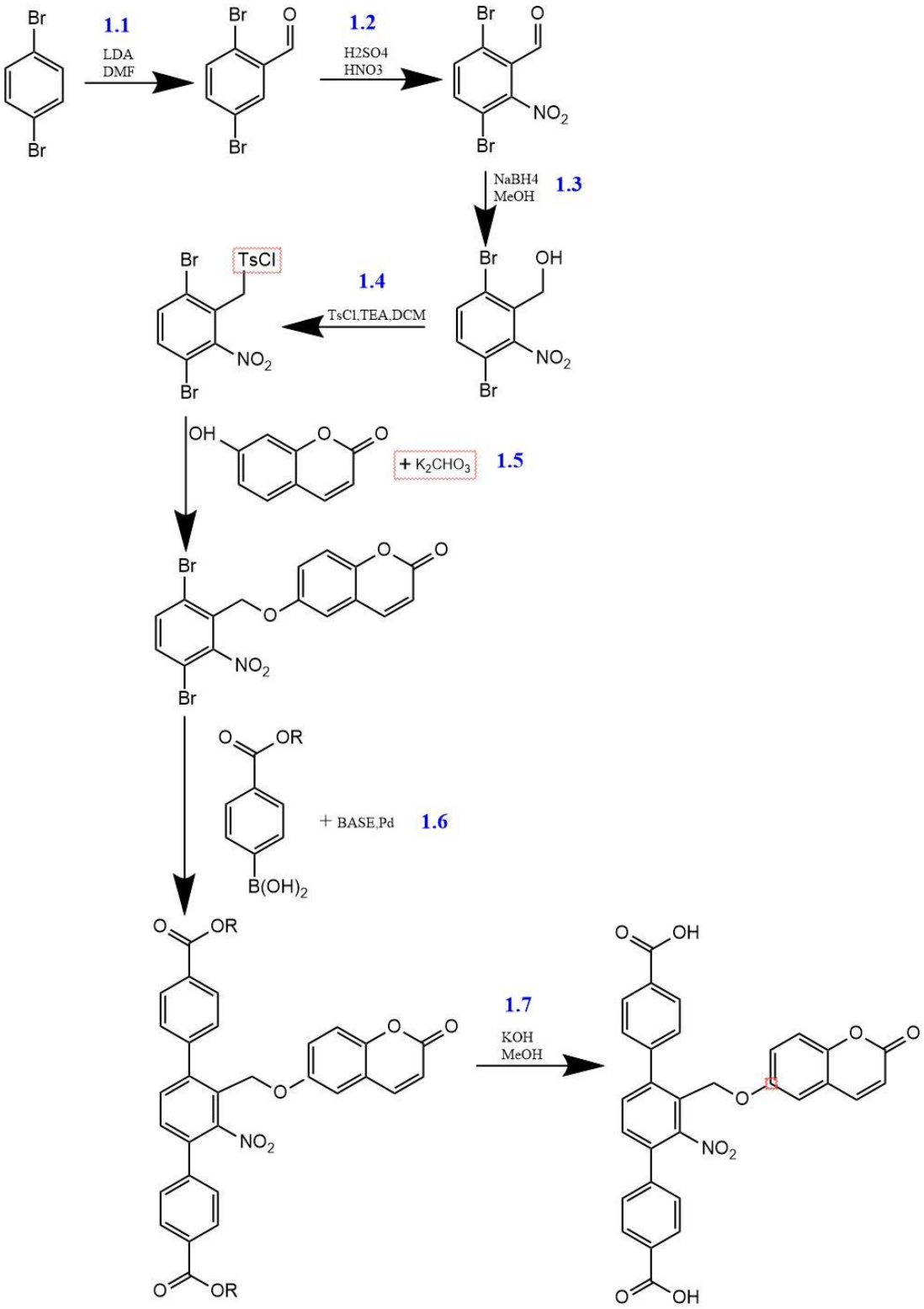

Figure 8: Proposed synthesis scheme for development of a linker capable of light-catalyzed drug release upon stimulation via UV light via an *ortho*-nitrobenzyl caging reaction.

CHAPTER FIVE: CONCLUSION

The objective of this work was the preparation of water-stable MOFs whose linkers are decorated with functional groups that have potential compatibility in drug delivery systems and to explore the efficacy of certain synthesis conditions in terms of the crystallinity of the MOF product. This work represents the first steps toward the development of MOFs featuring direct covalent attachment of anticancer drugs and fluorescent tags for their controlled release in the body. The results herein indicate the versatility of UiO MOFs in terms of the types of groups that might be incorporated and reaffirm the importance of defining specific synthesis conditions in order to achieve optimal purity and crystallinity. The targeted release mechanisms for which this research forms a basis represent new therapeutic possibilities within nanomedicine for the treatment of cancer. Such mechanisms as the light-triggered *ortho*-nitrobenzyl caging reaction confer a high degree of control over where and when the drug is released from the carrier MOF, which would allow for site-specific activation and reduce widespread damage to healthy tissues.

References

1. WHO | Cancer. *http://www.who.int/mediacentre/factsheets/fs297/en/* (accessed Apr 23, 2018).

2. Types of Cancer Treatment. *https://www.cancer.gov/about-cancer/treatment/types* (accessed Apr 24, 2018).

3. Gerlinger, M.; Rowan, A. J.; Horswell, S.; Larkin, J.; Endesfelder, D.; Gronroos, E.; Martinez, P.; Matthews, N.; Stewart, A.; Tarpey, P.; Varela, I.; Phillimore, B.; Begum, S.; McDonald, N. Q.; Butler, A.; Jones, D.; Raine, K.; Latimer, C.; Santos, C. R.; Nohadani, M.; Eklund, A. C.; Spencer-Dene, B.; Clark, G.; Pickering, L.; Stamp, G.; Gore, M.; Szallasi, Z.; Downward, J.; Futreal, P. A.; Swanton, C. Intratumor heterogeneity and branched evolution revealed by multiregion sequencing. *The New England Journal of Medicine* **2012**, *366*, 883.

4. Zugazagoitia, J.; Guedes, C.; Ponce, S.; Ferrer, I.; Molina-Pinelo, S.; Paz-Ares, L. Current Challenges in Cancer Treatment. *Clinical Therapeutics* **2016**, *38*, 1551-1566.

5. Jabir, N.R.; Anwar, K.; Firoz, C.K.; Oves, M.; Kamal, M.A.; Tabrez, S. An overview on the current status of cancer nanomedicines. *Current Medical Research and Opinion* **2018**, *34*, 911-921.

6. Keskin, S.; Kizilel, S. Biomedical Applications of Metal–Organic Frameworks. *Industrial Engineering and Chemistry Research* **2011**, *50*, 1799-1812.

7. Hiroyasu Furukawa; Kyle E. Cordova; Michael O'Keeffe; Omar M. Yaghi The Chemistry and Applications of Metal-Organic Frameworks. *Science* **2013**, *341*, 1230444.

8. Rowsell, J. L. C.; Yaghi, O. M. Metal–organic frameworks: a new class of porous materials. *Microporous and Mesoporous Materials* **2004**, *73*, 3-14.

9. Lazaro, I. A.; Forgan, R. S. Application of zirconium MOFs in drug delivery and biomedicine . *Coordination Chemistry Reviews* **2018**, *380*, 230-259.

10. Lan, G.; Ni, K.; Lin, W. Nanoscale metal–organic frameworks for phototherapy of cancer. *Coordination Chemistry Reviews* **2019**, *379*, 65-81.

11. Chauhan, A. Powder XRD Technique and its Applications in Science and Technology. *Journal of Analytical & Bioanalytical Techniques* **2014**, *5*, 1-5.

12. How an FTIR Spectrometer Operates. *https://chem.libretexts.org/Core/Physical_and_Theoretical_Chemistry/Spectroscopy/Vibrational_Spectroscopy/Infrared_Spectroscopy/How_an_FTIR_Spectrometer_Operates* (accessed Apr 24, 2018).

13. Katz, M. J.; Brown, Z. J.; Colon, Y. J.; Siu, P. W.; Scheidt, K. A.; Snurr, R. Q.; Hupp, J. T.; Farha, O. K. A facile synthesis of UiO-66, UiO-67 and their derivatives. *Chemical Communications (Cambridge, England)* **2011**, *48*, 19-22.

14. Mewes, J.; Neumann, K.; Verhoefen, M.; Wille, G.; Wachtveitl, J.; Dreuw, A. Molecular mechanism of uncaging CO2 from nitrophenylacetate provides general guidelines for improved ortho-nitrobenzyl cages. *Chemphyschem: A European Journal of Chemical Physics and Physical Chemistry* **2011**, *12*, 2077-2080.

15. Mewes, J.; Dreuw, A. On the role of singlet versus triplet excited states in the uncaging of ortho-nitrobenzyl caged compounds. *Physical Chemistry and Chemical Physics* **2012**, *1*, 6691-6698.